

## Three Dimensional Particle Simulation of High Altitude Rocket Plumes

Leonardo Dagum<sup>1</sup> and S.H. Konrad Zhu<sup>2</sup>

Report RNR-92-026, September 4, 1992

*Presented at AIAA 27<sup>th</sup> Thermophysics Conference, July 6-8, 1992, Nashville, TN, paper AIAA 92-2913.*

NASA Ames Research Center  
Moffett Field, CA 94035

September 4, 1992

### Abstract

*The interaction of two nozzles exhausting into vacuum generates a complex three-dimensional shock structure. The shock structure and resulting plume flow field is characterized by the nozzle separation distance. For the appropriate range of penetration Knudsen numbers, the analysis of this shock structure can be suitably accomplished through a Monte Carlo simulation. This paper describes the application of a general three-dimensional Monte Carlo simulation on the Connection Machine CM-2 to the analysis of the plume self-interaction shock in the near field. Results are presented for two cases, corresponding to a small and a large nozzle separation distance. The results correctly reproduce the expected flow features and demonstrate the ability of this method to properly simulate the start of the plume self-interaction shock. This has significance not only for allowing analysis of the self-interacting plume in the near field, but also for allowing the subsequent simulation of the far field flow through the use of a continuation downstream exit boundary.*

---

<sup>1</sup>Employee of Computer Sciences Corp, Work sponsored under NASA contract NAS-2-12961

<sup>2</sup>Employee of Rockwell International Corp. Canoga Park, CA 91303. Work sponsored under NASA contract NASA 8-251082

# Three Dimensional Particle Simulation of High Altitude Rocket Plumes<sup>1</sup>

Leonardo Dagum\*  
NASA Ames Research Center  
Moffett Field, CA 94035

S.H. Konrad Zhu†  
Rocketdyne Division  
Rockwell International Corp.  
Canoga Park, CA 91303

July 5, 1992

## Abstract

The interaction of two nozzles exhausting into vacuum generates a complex three-dimensional shock structure. The shock structure and resulting plume flow field is characterized by the nozzle separation distance. For the appropriate range of penetration Knudsen numbers, the analysis of this shock structure can be suitably accomplished through a Monte Carlo simulation. This paper describes the application of a general three-dimensional Monte Carlo simulation on the Connection Machine CM-2 to the analysis of the plume self-interaction shock in the near field. Results are presented for two cases, corresponding to a small and a large nozzle separation distance. The results correctly reproduce the expected flow features and demonstrate the ability of this method to properly simulate the start of the plume self-interaction shock. This has significance not only for allowing analysis of the

self-interacting plume in the near field, but also for allowing the subsequent simulation of the far field flow through the use of a continuation downstream exit boundary.

## 1 Introduction

High altitude rocket plumes are of great interest to the spacecraft designer. The impingement of rocket plumes on the exterior of spacecraft, in particular the solar panels, can lead to problems either from contamination, control, or even structural integrity. The current work is prompted by the space station design and the possible problems due to the Orbiter reaction control system (RCS) plumes impinging on the space station solar panels. In order to predict the gas-surface interaction at the solar panel it is necessary to have an accurate description of the RCS plume flowfield.

The Orbiter RCS consist of 44 engines, of which 38 are the primary engines with nominal thrust of 870 lbf and the rest are vernier engines of 25 lbf thrust. One of the major problem in the space station design is to accurately predict the RCS plume loads on the Photovoltaic(PV) array during the proximity operation of the Orbiter in the vicinity of the

\*Employee of Computer Sciences Corp., member AIAA. Work sponsored under NASA contract NAS-2-12961

†Member AIAA. Work sponsored under NASA contract NASA 8-251082

<sup>1</sup>Copyright ©1992 by Leonardo Dagum and S.H. Konrad Zhu. Published by the American Institute of Aeronautics and Astronautics, Inc. with permission.

space station. Since the complex maneuvering in the proximity operation demands a myriad of cases of the RCS engine firings, to predict the resultant plume flowfield is a formidable task. One of the difficulties is to predict the plume flowfield generated from multiple RCS engine firings. The spacing between RCS engine locations in multiple firings range from under a meter to approximately 30 meters. Any combination of the engines to be fired are possible in the maneuvering, of course, those symmetrical with respect to the axes of the Orbiter are most likely to be used. Considering the engine thrust level and the range of the spacing, it is obvious that attempts to solve this problem either by numerical simulation or by experimental means are very challenging.

This paper describes a simulation method for accurately describing general, three dimensional high altitude rocket plumes and multiple plume interactions. The results presented here are from the initial phase investigation in a study of the Orbiter RCS engine exhaust plume. The simulation method has demonstrated the capability to capture important flow features resulting from two identical plumes separated by a given distance, especially in the intriguing region of high off-center angle from the nozzle center line, where the flow rarefaction and on-set of the shock formation due to the plume self-interaction are intricately entwined.

At high altitudes, rarefaction effects in the rocket exhaust plume become important and continuum approaches toward simulation no longer apply. Since the space station will orbit the earth at 350-460 km altitude, the RCS engines essentially will be exhausting to vacuum. At the nozzle exit plane the flow is not considered rarefied (except at the nozzle lip), but through rapid expansion to vacuum rarefaction effects appear in the near field.

The self-interaction shock is the topic of concern in [1], where an axisymmetric approx-

imation is used to reduce the complexity of the problem. The important conclusion from this paper is that self-interaction shocks may be of concern even at a Knudsen number of 0.00757 (based on the nozzle separation distance) and superposition of point sources is not accurate at Knudsen numbers below this value.

The current work also focuses on the plume self-interaction problem, however with a fully three-dimensional simulation. The objective is to accurately capture the complex three-dimensional near field flow features of the plume and self-interaction shock. Since the shock originates in the near field, the near field solution can be used later to calculate the far field solution. However, it is impossible to accurately simulate the far field without including effects from the flow at large off-center (from the nozzle axis) angles which comprise the near field solution.

## 2 Computational Technique

The current work makes use of a particle simulation code written in CM Fortran for the Connection Machine CM-2. The implementation is described in detail in [2, 3, 4]. The original code was enhanced with two additional capabilities in order to more efficiently simulate plume flow fields. These capabilities are described in below.

### 2.1 Dynamic Array Resizing

In addition to particle cloning [5] the current code allows for dynamic array resizing. This permits the array sizes to be doubled without also doubling the number of particles. This feature is used during the transient part of the flow and allows the simulation to be started with small array sizes which then grow as the number of particles in the simulation grows. This is of importance on the Connection Machine CM-2 because of its single in-

struction multiple data stream (SIMD) architecture. Every instruction on the CM-2 effectively gets executed once for every element of the array which the processors are referencing. This is true even when most of the elements in an array have been masked off. Therefore it is very important, in terms of computational performance, to make the array sizes comparable to the number of particles in the flow.

## 2.2 Starting Solution

The simulation space effectively begins at a sphere of some arbitrary radius from the nozzle exit plane center. The starting conditions are loaded as a starting line solution typically obtained from a method of characteristics nozzle code. This solution is assumed to be strictly a function of the off-center angle,  $\theta$ . Figure 1 presents the general configuration for the simulation of the plume self-interaction shock. This figure is a schematic of the plane joining the two nozzle axes. The simulation space is bounded by the box ABCD, with the nozzle axis lying outside of the simulation. The boundary at BC is specularly reflecting and therefore produces an image nozzle on the opposite side. The boundaries AB, AD, and CD are vacuum boundaries such that any particles crossing these boundaries are removed from the simulation. Particles are introduced along the starting line FG as will be described. One specifies a minimum starting angle for the simulation. Note that to the left of the line FH is vacuum, and there is some diffusion of particles into the smaller angles left of FH. The assumption made is that the Mach number at the starting line is sufficiently high that the actual amount of diffusion will be small and thus have no influence on the solution at greater angles from the nozzle exit plane center at E. The displacement EB is adjustable and measures half the separation distance for the two nozzles. Moving the nozzle exit plane center

to B (i.e. setting EB to zero) allows the simulation of a single nozzle plume flowfield.

When the simulation begins the space is empty. Particles are introduced at some fixed rate every time step. The starting line density, temperature, and speed are loaded into lookup tables and each particle's angular position is chosen randomly by using the acceptance-rejection method to sample from the given exit plane density distribution. The corresponding bulk speed and temperature is then looked up. The particle's thermal velocity is sampled from a Maxwellian distribution at the given temperature. The particle's bulk velocity is determined by decomposing the bulk speed into the three coordinate directions.

## 3 Physical Modelling

The parameters describing the RCS rocket engines are given in table 1. Although these engines use MMH/NTO as a propellant, the simulations were carried out assuming molecular nitrogen as the exhaust gas. Physical models for particle simulation of molecular nitrogen are well established, and this simplification allowed the development of the code to proceed without requiring new physical models to be developed. The variable hard sphere collision model is used with an inverse ninth-power for the force law. This results in a coefficient of viscosity,  $\mu$ , proportional to  $T^{0.72}$ , the accepted result for nitrogen. The Borgnakke-Larsen model is used to model internal energy with collision numbers fixed at 5 for rotation and 50 for vibration.

## 4 Results

The length scale in this flow field is defined by the separation distance between the two nozzles (i.e. twice the distance EB in figure 1). Results are presented for separation distances

Parameter	PRCS	Simulated
Propellant	MMH/NTO	$N_2$
Mixing Ratio	1.63	N/A
Expansion Ratio	22.	22.
Chamber Press (psi)	153	153
Chamber Temp ( $^{\circ}$ R)	5710	4859
Thrust (lbf)	870	848
Mass Flow Rate (lbm/sec)	2.809	3.627
Ratio of Specific Heats (after nozzle expansion)	1.28	1.37

Table 1: Orbiter PRCS engine and simulated engine parameters.

of 18.5 m and 7.8 m. The pertinent parameters for the two simulation runs are given in table 2. The starting surface for particles is at 3.09 m from the nozzle exit plane center. The starting line conditions were obtained from the method of characteristics code RAMP2 using molecular nitrogen as a propellant (see [6]) under the conditions given by table 1. Figure 2 presents the starting line density as a function of the off-center angle. Figures 3 and 4 present the starting line temperature and bulk speed.

## Case 1

Grid dimensions	$53 \times 135 \times 53$
Minimum $\theta$	$20^{\circ}$
Separation distance	119.7 cells
Starting line radius	20.0 cells

## Case 2

Grid dimensions	$46 \times 135 \times 46$
Minimum $\theta$	$20^{\circ}$
Separation distance	126.0 cells
Starting line radius	50.0 cells

Table 2: Simulation parameters for 18.5 m (case 1) and 7.8 m (case 2) separation distances.

A useful measure of the degree of rarefaction is given by the *penetration* Knudsen number,

$Kn_p$ , defined as (see [7])

$$Kn_p = \lambda_{12}/L \quad (1)$$

where  $\lambda_{12}$  is the mean distance which a particle from plume 1 travels between two successive collisions with particles from plume 2; and the reference length  $L$  is given by  $d/(2 \sin \theta)$  where  $d$  is the separation distance between the two nozzles. The penetration Knudsen number along the interaction plane was computed using an appropriate source flow model (see [6]) and the results are shown in figure 5. Note that the two cases considered lie largely in the range  $0.01 < Kn_p < 1$  which represents the transition regime between the continuum and free molecule limits. This result indicates that particle simulation is appropriate.

Case 1 is the large separation distance of 18.5 m. Figure 6 presents the density contours (in  $\text{kg/m}^3$ ) in the plane joining the two nozzles. One can see evidence of the self-interaction shock beginning about the 45 degree off-center angle (remember the nozzle axis is 6.8 cells to the left of the simulation space) which corresponds to a distance of 9.3 m from the nozzle exit plane, or approximately half the separation length  $d$ . The simulation space extends only about one separation length downstream from the nozzle exit plane, which is insufficient to allow any appreciable

curvature in the self-interaction shock. The simulation space covers off-center angles from 20 to 90 degrees, however most of the mass is in the 0 to 20 degree region (see figure 2), and one would expect the shock to move away from the interaction plane only when the influence of gas from those smaller off-center angles is felt.

Figure 7 presents the translational temperature contours (in kelvins) for the same plane as figure 6. One can see a stagnation region in the vicinity of 70 to 90 degrees. This region is highly rarefied (see figure 5) and the number of particles is comparatively small. For this reason the solution here has a relatively large statistical uncertainty associated with it. Nonetheless, it is possible to more precisely assess the location of the stagnation point by examining the velocity field in conjunction with the temperature field in this region. Figure 8 presents the velocity field in the stagnation region along with the temperature contours at 2200 °K and 4900 °K. The stagnation point appears to occur approximately 7 cells above the nozzle exit plane, which corresponds to a distance of 1.1 m (5.8 % of a separation length) or at an off-center angle of 83 degrees. Note that at this off-center angle the penetration Knudsen number is greater than 1 and it is not clear that a stagnation point may be defined. One could more accurately resolve the stagnation region by running the simulation starting with a greater minimum angle than the 20 degrees used here, however that trades off on the downstream distance which can be covered.

Figure 9 presents the rotational temperature contours (in kelvins) for the same plane as figure 6. One can see the expected lag in the rotational temperature over translational temperature, with the peak rotational temperature occurring somewhat downstream of the stagnation point. Vibrational temperature fields are not presented as, for the most part,

vibrational energies are not excited and what little evidence of vibrational energy appears has associated with it a large amount of statistical noise.

Case 2 is the small separation distance of 7.8 m. Figures 10 through 13 are correspond to figures 6 through 9 for the small separation case. The cell dimensions for this case are smaller than for case 1. Looking at figure 10, again first evidence of the self-interaction shock appears around the 45 degree off-center angle. The flow features are very similar to those of case 1, however the self-interaction shock now is sharper because of the lower Knudsen number. The translational temperature contours are given in figure 11 and the velocity field in the stagnation region is given in figure 12. The stagnation point appears to occur approximately 16 cells above the nozzle exit plane, which corresponds to an off-center angle of 76 degrees. With the closer separation distance, more mass flows backwards therefore one expects the stagnation point to move forwards in this manner. Note however, that for both case 1 and case 2 the penetration Knudsen number at the high off-center angles is greater than 1, and a proper stagnation point may not exist. Greater resolution of the stagnation region is necessary before any conclusions may be drawn on this matter.

The rotational temperature contours are presented in figure 13. Again the lag in rotation over translation is evident.

The three dimensional nature of the self-interaction shock is made evident in figures 14 through 16. These figures present density contours on planes parallel to the nozzle exit plane at downstream displacements of 3.9 m, 5.85 m, and 7.8 m (or  $0.5d$ ,  $0.75d$ , and  $1d$  respectively). The interaction plane is at the top of each figure, and the contours at the bottom delimit the vacuum where no particles were introduced. Note that as you move away from the plane containing the two nozzle axes (i.e.

the left hand border of figures 14-16), the minimum off-center angle for input particles increases, and this accounts for the curvature of the vacuum boundary marked by the contours at the bottom of the figure. At 3.9 m the self-interaction shock is not clearly visible with the contours shown, but the structure of the plume is well defined and clearly is expanding radially from the origin at the nozzle exit plane center. At 5.85 m the self-interaction shock is clearly evident along with the plume structure. The shock strength decreases going away from the plane containing the two nozzle axes. At 7.8 m this reduction in shock strength is more clearly evident, but very little of the plume structure remains since at this displacement the plume is contained in off-center angles less than 20 degrees.

## 5 Performance

The results presented above were computed using only 16k processors of the 32k processor Connection Machine CM-2 in the Numerical Aerodynamic Simulation facility at the NASA Ames Research Center. The time step for the simulations were rather small in order to obtain the correct collision frequency. The starting line conditions (see figures 2 to 4) correspond to very low Knudsen numbers and are difficult to meet. For this reason, a large number of time steps were required to reach steady state (typically about 4500 steps were taken). Particle cloning was employed to help speed the transient by using less particles to establish the steady state, however care was taken to eliminate any residual statistical dependencies from cloning by taking at least 100 steps between subsequent clonings. The steady state calculations employed about 4 million particles and were averaged for about 1000 steps each (samples were collected on every time step). The average CPU time per step

during the time averaging phase was 23 seconds. In all, each calculation required about 8 hours to complete. Clearly, this kind of calculation is not a "showboat" heroic effort but rather something which can be carried out on a fairly routine basis for engineering analysis purposes.

## 6 Conclusions

The interaction of two nozzles exhausting into vacuum generates a complex three-dimensional shock structure. The shock structure and resulting plume flow field is characterized by the nozzle separation distance. For the appropriate range of penetration Knudsen numbers, the analysis of this shock structure can be suitably accomplished through a Monte Carlo simulation. This paper describes the application of a general three-dimensional Monte Carlo simulation on the Connection Machine CM-2 to the analysis of the plume self-interaction shock in the near field. Results are presented for two cases, corresponding to a small and a large nozzle separation distance. The results correctly reproduce the expected flow features and demonstrate the ability of this method to properly simulate the plume self-interaction problem.

Although the results presented are limited to just the near field (up to one nozzle separation length) solution, they do allow the calculation of the far field solution through the use of a continuation boundary at the downstream exit plane. In other words, one can carry out the far field simulation by using the starting solution only for the small off-center angles and using the exited particles from the near field simulation to couple the influence to the flowfield from the large off-center angles. Since the large off-center angles fix the stagnation point and determine the position of the self-interaction shock, it is not possible

to accurately simulate the far field without including effects from the large off-center angle flow and near field solution.

## References

- [1] Hermina, W., *Direct Simulation Monte Carlo Model for Space Vehicle Plume Environments*, Sandia National Laboratories Report SAND88-8827, 1988.
- [2] Dagum, L., *On the Suitability of the Connection Machine for Direct Particle Simulation*, Dept Aeronautics and Astronautics Ph.D. Thesis, Stanford University, Stanford, CA, 1990.
- [3] Dagum, L., *Three Dimensional Direct Particle Simulation on the Connection Machine*, AIAA-91-1365, 1991.
- [4] Dagum, L., *Data Parallel Sorting for Particle Simulation*, Concurrency: Practice and Experience, (to appear) 1992.
- [5] McDonald, J.D., *A Computationally Efficient Particle Simulation Method Suited to Vector Computer Architectures*, Ph.D. Thesis, Dept Aero and Astro, Stanford Univ, Stanford, CA, 1989.
- [6] Zhu, S.K., and Clack, H., *Comparison Between Plume Flowfield Predictions Made by the RCSFORCE and the MOC Based Codes* Rocketdyne Internal Letter, AFD-92-012, April 1992.
- [7] Koppenwallner, G., *Scaling Laws for Rarefied Plume Interference with Application to Satellite Thrusters*, 14<sup>th</sup> International Symposium on Space Technology and Science, Tokyo, Japan, May 28 - June 2, 1984.

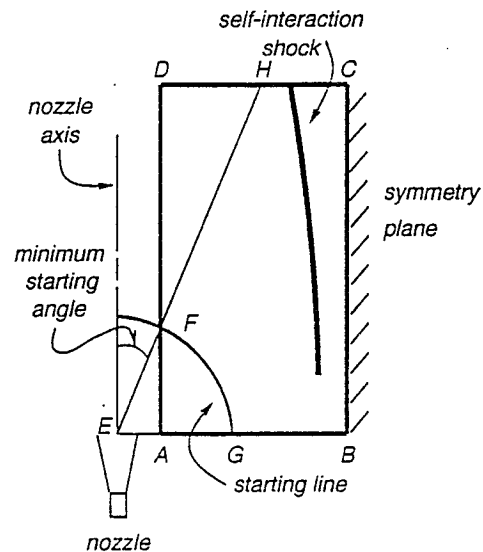


Figure 1: General configuration for the simulation of the plume self-interaction shock.

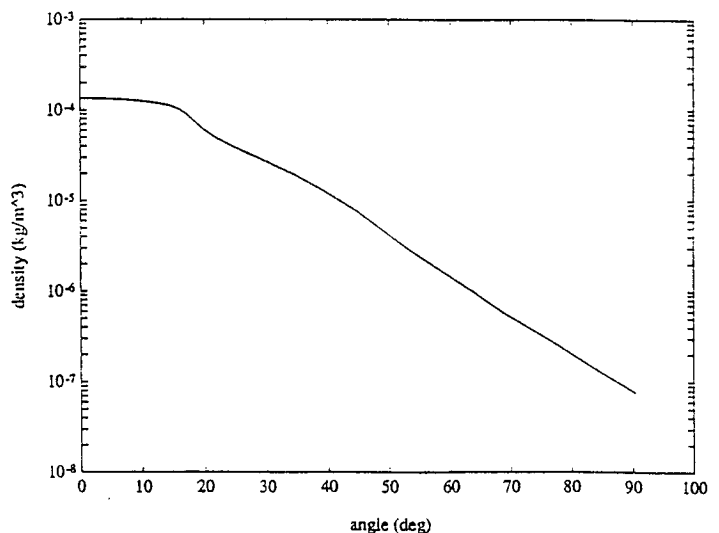


Figure 2: Starting line density.



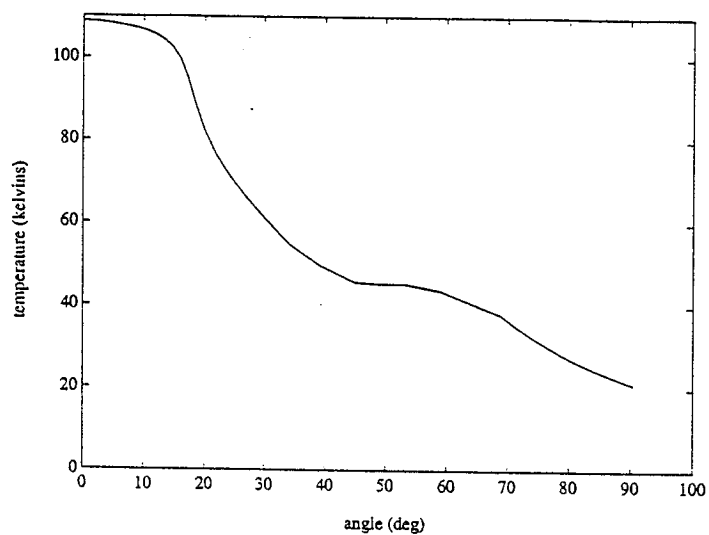


Figure 3: Starting line temperature.

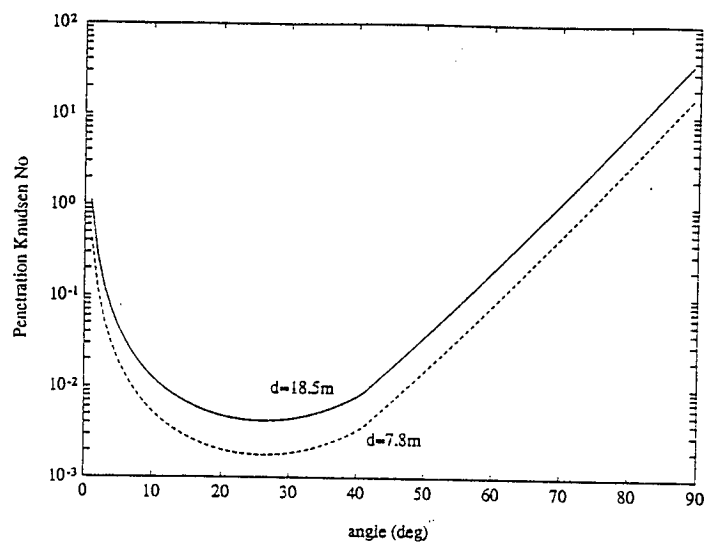


Figure 5: Penetration Knudsen number along the interaction plane for 7.8 m and 18.5 m nozzle separation distances.

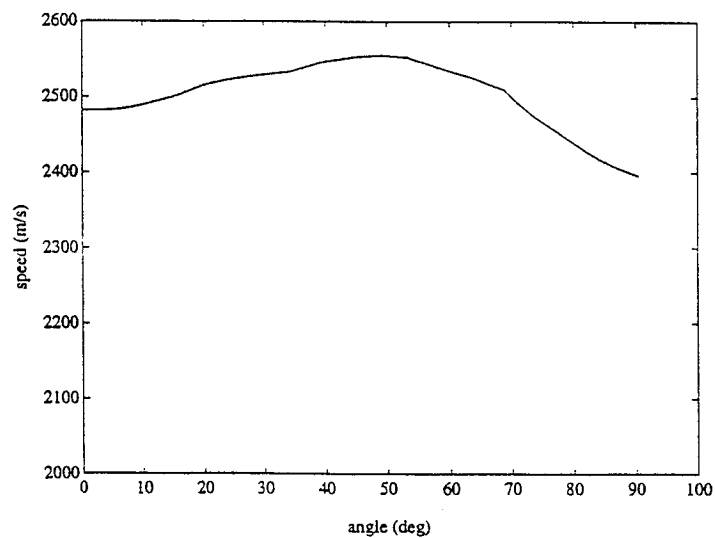
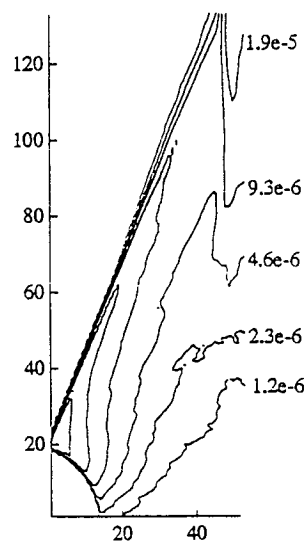


Figure 4: Starting line bulk speed.

Figure 6: Density contours for 18.5 m separation distance (units of  $\text{kg/m}^3$ ).

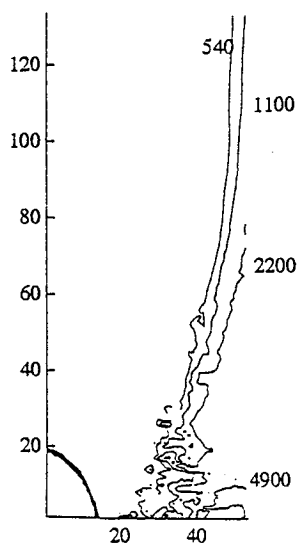


Figure 7: Translational temperature contours for 18.5 m separation distance (units of kelvins).

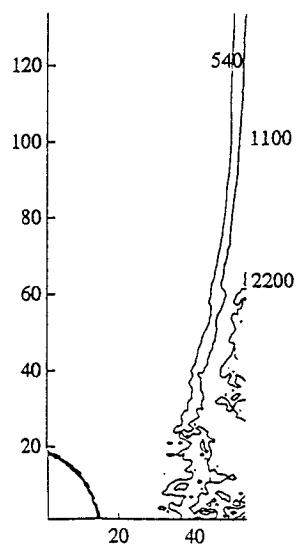


Figure 9: Rotational temperature contours for 18.5 m separation distance in the stagnation region (units of kelvins).

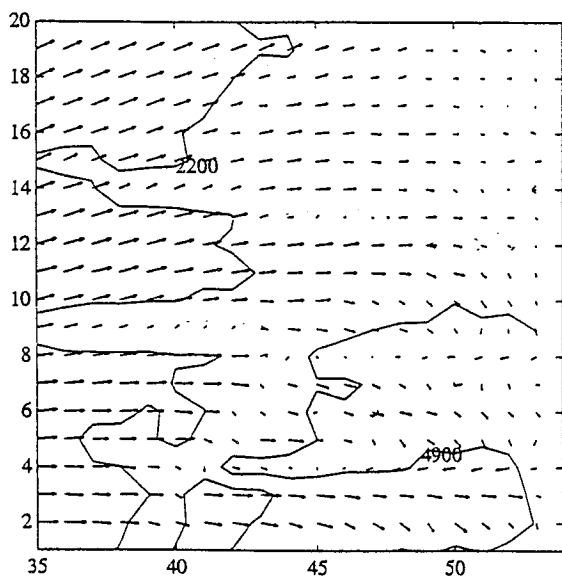


Figure 8: Velocity and translational temperature field for 18.5 m separation distance in the stagnation region (units of kelvins).

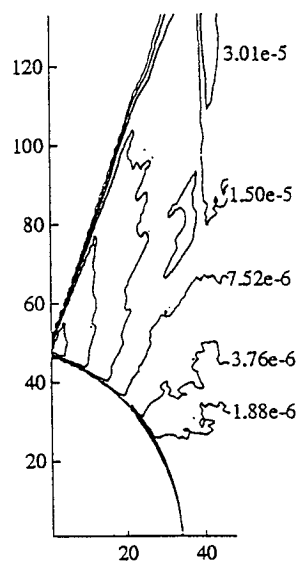


Figure 10: Density contours for 7.8 m separation distance (units of  $\text{kg/m}^3$ ).

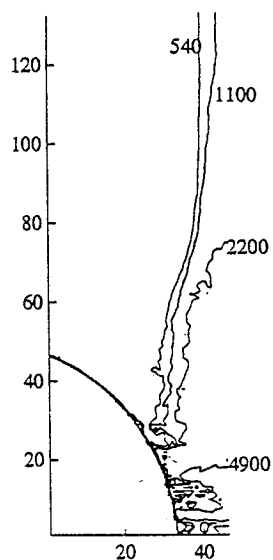


Figure 11: Translational temperature contours for 7.8 m separation distance (units of kelvins).

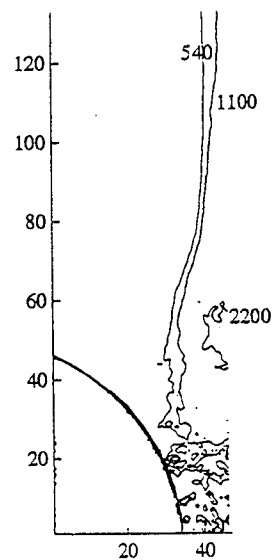


Figure 13: Rotational temperature contours for 7.8 m separation distance in the stagnation region (units of kelvins).

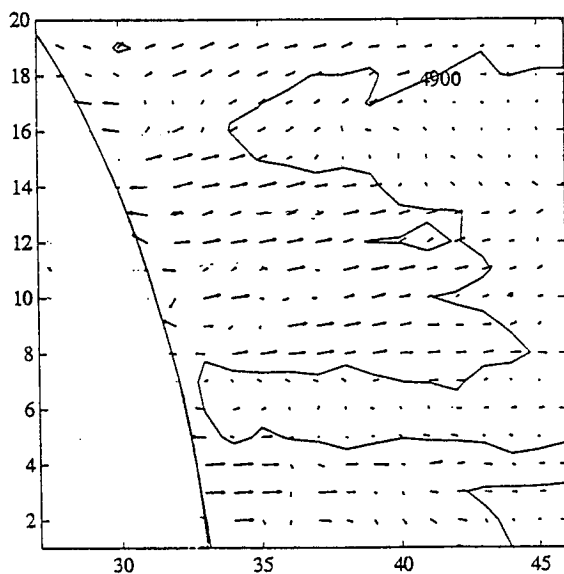


Figure 12: Velocity and translational temperature field for 7.8 m separation distance in the stagnation region (units of kelvins).

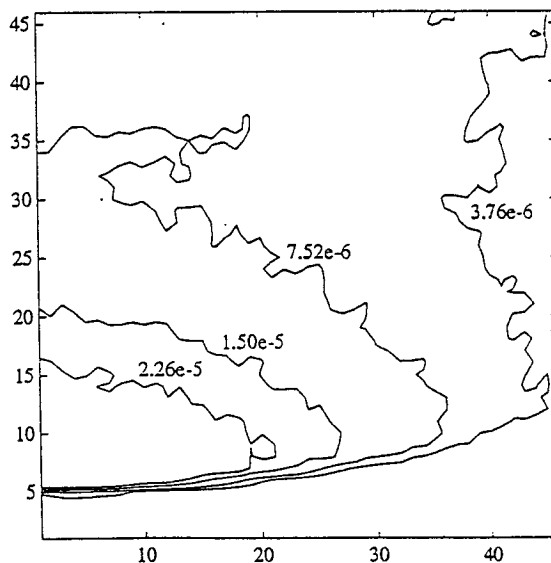


Figure 14: Density contours for 7.8 m separation distance at 3.9 m downstream of the nozzle exit plane (units of  $\text{kg/m}^3$ ).

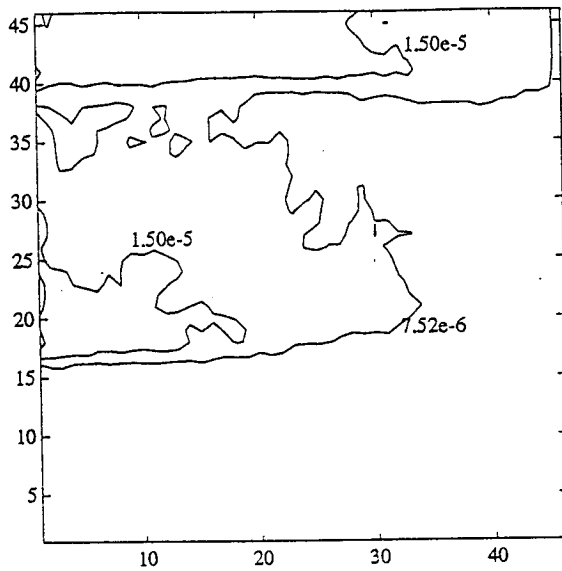


Figure 15: Density contours for 7.8 m separation distance at 5.85 m downstream of the nozzle exit plane (units of  $\text{kg/m}^3$ ).

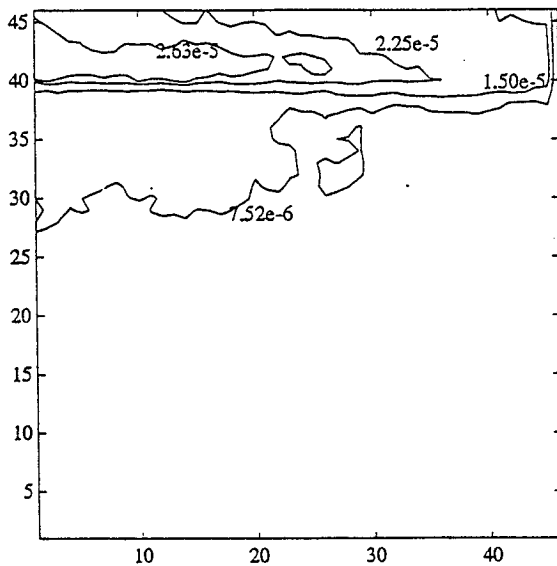


Figure 16: Density contours for 7.8 m separation distance at 7.8 m downstream of the nozzle exit plane (units of  $\text{kg/m}^3$ ).